MODELOWANIE INŻYNIERSKIE ISSN 1896-771X
39, s. 81-88, Gliwice 2010

HIGH-FREQUENCY MODEL OF MONOTUBE SHOCK ABSORBERS

JANUSZ GOŁDASZ

BWI Group, Technical Center Kraków, ul. Podgórki Tynieckie 2, 30-399 Kraków, PL
e-mail: janusz.goldasz@bwigroup.com

Summary. It has been long recognized that the inertia and compressibility of the fluid have an impact on the dynamic behaviour of semi-active monotube shock absorbers utilizing so-called smart ER/MR fluids at high frequencies of the system operation. Previous studies which dealt with analytical state-space & CFD models of the magnetorheological shock absorber in a monotube configuration indicated that any conventional analytical model is lightly damped and not suitable for dynamic studies above 100-150 Hz. Therefore, in the present paper the author illustrates an analytical model of a monotube shock absorber that is suitable for high-frequency studies. In particular, the study presents a comparison between the CFD results and the new model. Finally, the shock absorber characteristics in the form of Bode plots of amplitude and frequency are presented within a prescribed range of frequencies.

1. INTRODUCTION

Investigation of the dynamic behavior of Magneto-Rheological (MR) & Electro-Rheological shock absorbers [5,6,7] subjected to a small-stroke, medium- to high-frequency excitation has revealed some interesting characteristics best described as a clockwise rotation of the damping force vs. displacement characteristic curves ("ellipses") with increasing stroking frequency. The same phenomenon is responsible for the hysteretic behavior seen in the force vs. piston velocity characteristic curves as shown in Figures 1 and 2. In Reference [1] the author makes the hypothesis that the likely contributors is the fluid inertia and the compressibility, and describes a fairly detailed force-driven model of the damper incl. the compressibility of fluid chambers, laminar losses through the piston annular flow path, and the inertia of the fluid element occupying the annulus. Both piston and rod assembly (P&R) inertia were taken into account. The numerical calculation carried out in [1] identified two vibration modes. The primary one relates to the fluid element dynamic, whereas the second (higher) resonant frequency is due to the combined inertia of the P&R and the fluid element. As a result, in Reference [2] an observation was made that the P&R inertia has little or no effect under normal working conditions, and can be eliminated leading to a simplified reduced order stroke-driven model that describes adequately the MR damper dynamics for frequencies up to the first natural frequency of the damper.

The purpose of the present study is to extend the earlier analytical model for the simplest model configuration presented in Reference [2], and further analyzed in Reference [3] against Computational Fluid Dynamics (CFD) data. When compared against the CFD results, it became clear the analytical model of [2] would be lightly damped at the higher frequency

regime, and a mechanism for accounting for the viscosity (and the inertia) of the fluid throughout the damper should be investigated and added to the analytical models in order to improve its fidelity at frequencies near the resonance. As such, in the present paper a hydraulic network type model of a shock absorber is designed and tested in order to confirm the CFD study conclusions. Therefore, in Section 2.1 the author outlines the hydraulic network approach and the dynamic model of the shock absorber, and Section 2.2 contains details of the CFD experiment performed by the author in order to test the network model. Sections 2.3 and 2.4 contain damper configuration specific data and damper test setup information, respectively. Finally, the results are presented in Section 2.5 and the conclusions drawn in Section 3.

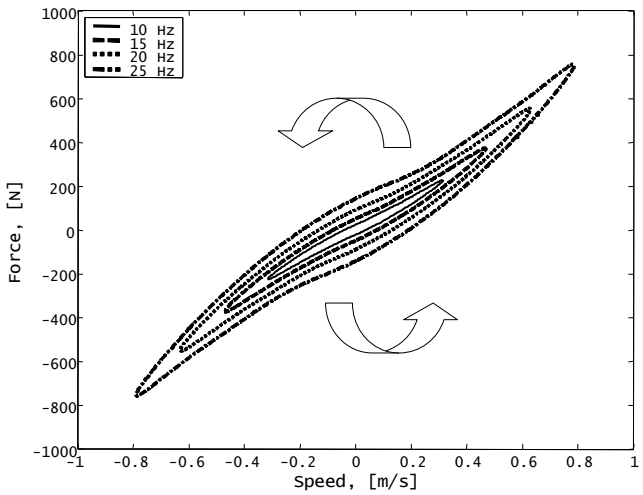

Figure 1. Off-state (zero current) force-velocity phase plane

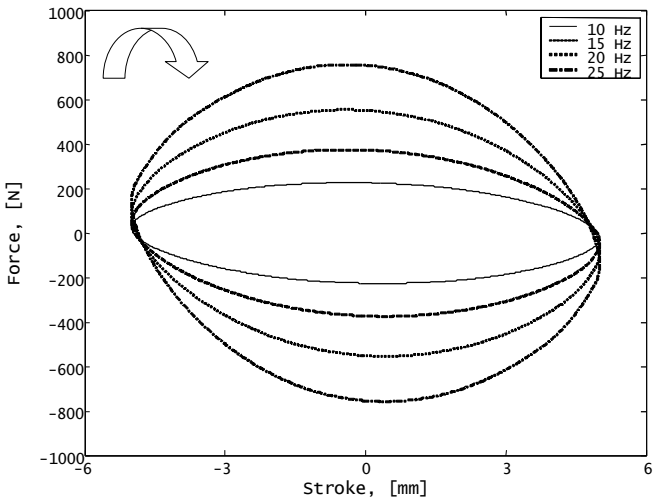

Figure 2. Off state force-displacement phase plane

2. MODELING AND SIMULATIONS

2.1. Shock absorber model

Consider the monotube damper configuration shown in Figure 3 and the simplified configuration in Figure 4. The cylinder tube houses the floating piston (gas cup) which separates the fluid from the pressurized gas. The main piston separates the upper and lower fluid chambers and includes an annular passage to permit the fluid to flow from one chamber to the other. In the present study the annulus is approximated by flat-plate geometry of length (area) L_g (A_g). The shock absorber fluid is characterized by the three parameters: the density ρ, the bulk modulus β, and the viscosity μ; the magnetic field is absent, and the fluid behavior is Newtonian. Therefore, the fluid flow through the annulus produces viscous damping forces.

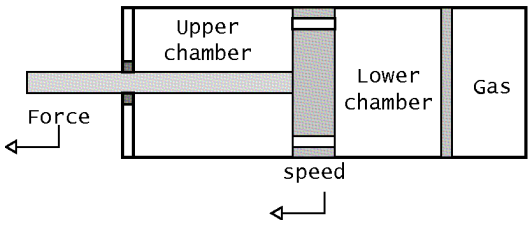

Figure 3. Monotube damper configuration [1]

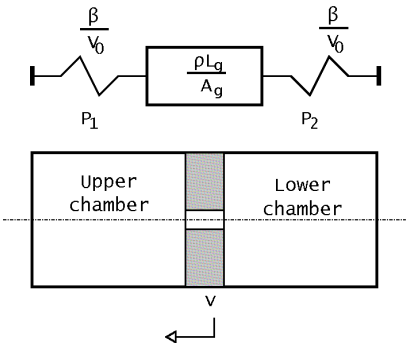

Figure 4. Reduced (velocity-driven) damper configuration
and its lumped parameter model [2]

In order to account for the viscous losses across the whole shock absorber volume, the fluid volumes on either side of the main piston were modeled as a hydraulic network of inertia, compliance and viscous resistance elements. Figure 5 shows the lumped parameter approximation of mass-spring portion of the (compliant) fluid volume. The inertia factor of a single lump of length L_i (and the volume $V_{0,i}$) is then equal to $\rho L_i/A_i$, whereas the compliance of the lump is $\beta/V_{0,i}$. The annulus cross-sectional area is A_i. .Then, the corresponding equations of motion for the lump i at mid-stroke conditions are as follows

$$\begin{cases} \dfrac{dQ_i}{dt} = \dfrac{A_i}{\rho L_i}\left(P_{in} - P_{out} - R_i Q_i\right) \\ \dfrac{dP_{in}}{dt} = \dfrac{\beta_i}{V_{0,i}}\left(Q_{in} - Q_i\right) \\ \dfrac{dP_{out}}{dt} = \dfrac{\beta_i}{V_{0,i}}\left(Q_i - Q_{out}\right) \end{cases} \tag{1}$$

$$R_i = \frac{128\mu L_i}{\pi d_i^4} \tag{2}$$

where P_{in}, P_{out} are the pressures in and out of the lump, and Q_{in}, Q_{out} are the volume flow rates associated with the pressures, respectively. R_i accounts for the hydraulic resistance of the lump, and d_i refers to the lump hydraulic diameter. Assuming laminar flow losses, the term can be given by Equation 2. For example, the equations of motion of a model consisting of three lumps ($N=3$) can be described in the following manner

$$\begin{cases} \dfrac{dP_1}{dt} = \dfrac{\beta}{V_{0,1}}\left(-Q_1\right) \\ \dfrac{dQ_1}{dt} = \dfrac{A_1}{\rho L_1}\left(P_1 - P_2 - R_1 Q_1\right) \\ \dfrac{dP_2}{dt} = \dfrac{\beta}{V_{0,2}}\left(Q_1 + A_p v - Q_2\right) \\ \dfrac{dQ_2}{dt} = \dfrac{A_g}{\rho L_g}\left(P_2 - P_3 - R_p Q_2\right) \\ \dfrac{dP_3}{dt} = \dfrac{\beta}{V_{0,3}}\left(Q_2 - A_p v - Q_3\right) \\ \dfrac{dQ_3}{dt} = \dfrac{A_3}{\rho L_3}\left(P_3 - P_4 - R_3 Q_3\right) \\ \dfrac{dP_4}{dt} = \dfrac{\beta}{V_{0,4}}\left(Q_3\right) \end{cases} \tag{3}$$

where v is the input velocity of the piston. In the above model shown in Figure 6 the flow rates Q_2, Q_3 and the pressures P_2 and P_3, respectively, drive the motion of the fluid element contained in the annular gap of the main piston. The area of the piston is A_p. The remaining variables account for the behavior of the corresponding fluid lumps. Note the above equations correspond to the simplified shock absorber configuration with no gas chamber in Figure 4.

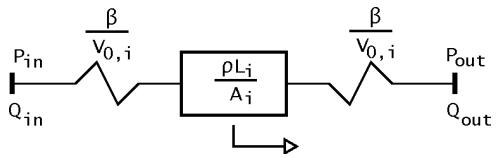

Figure 5. Hydraulic network lump

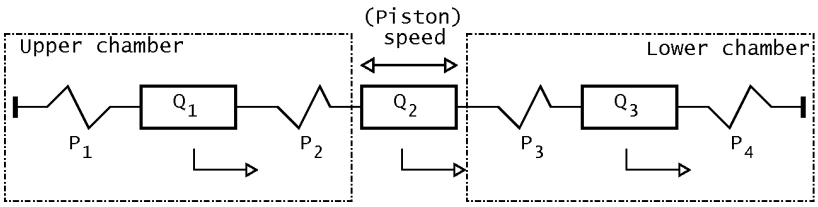

Figure 6. Hydraulic network model; N=3

As a result, the damping force across the piston can be obtained from

$$F_d = A_p\left(P_2 - P_3\right) \tag{4}$$

The equation set can be easily cast into the state-space form, thus yielding

$$\frac{dX}{dt} = AX + Bv \tag{5}$$

where $X = \left[P_1 \quad P_2 \quad P_3 \quad P_4 \quad Q_1 \quad Q_2 \quad Q_3\right]^T$. Therefore,

$$A = \begin{vmatrix} 0 & 0 & 0 & 0 & -\frac{\beta}{V_{0,1}} & 0 & 0 \\ 0 & 0 & 0 & 0 & \frac{\beta}{V_{0,2}} & -\frac{\beta}{V_{0,2}} & 0 \\ 0 & 0 & 0 & 0 & 0 & \frac{\beta}{V_{0,3}} & -\frac{\beta}{V_{0,3}} \\ 0 & 0 & 0 & 0 & 0 & 0 & \frac{\beta}{V_{0,4}} \\ \frac{A_1}{\rho L_1} & -\frac{A_1}{\rho L_1} & 0 & 0 & -R_1\frac{A_1}{\rho L_1} & 0 & 0 \\ 0 & \frac{A_2}{\rho L_2} & -\frac{A_2}{\rho L_2} & 0 & 0 & -R_2\frac{A_2}{\rho L_2} & 0 \\ 0 & 0 & \frac{A_3}{\rho L_3} & -\frac{A_3}{\rho L_3} & 0 & 0 & -R_3\frac{A_3}{\rho L_3} \end{vmatrix} \tag{6}$$

$$B = \begin{vmatrix} 0 & 0 & 0 & 0 & 0 & 0 & 0 \\ 0 & 0 & 0 & 0 & \beta\frac{A_2}{V_{0,2}} & 0 & 0 \\ 0 & 0 & 0 & 0 & -\beta\frac{A_2}{V_{0,3}} & 0 & 0 \\ 0 & 0 & 0 & 0 & 0 & 0 & 0 \\ 0 & 0 & 0 & 0 & 0 & 0 & 0 \\ 0 & 0 & 0 & 0 & 0 & 0 & 0 \\ 0 & 0 & 0 & 0 & 0 & 0 & 0 \end{vmatrix} \tag{7}$$

from which the (linear) network transfer function between the output force and the input velocity can be easily deduced in an analytical fashion.

2.2. CFD model

The FLUENT unsteady 2D-axisymmetric model configuration shown in Figure 7 corresponds to the simple shock absorber model explored in [2] and shown in Figure 4; the reader should refer to the paper for further information. Shortly, the piston rod is neglected, and the piston motion is prescribed as a sinusoidal velocity profile to reflect the actual testing conditions of real dampers. In the analysis dynamic layering algorithm in FLUENT was used to adjust the model mesh according to the prescribed motion profile. Finally, the damping force was obtained by integrating pressure distributions on either side of the piston.

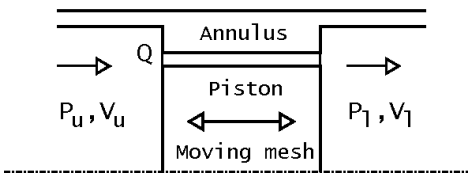

Figure 7. CFD monotube damper model
(only the annulus with adjacent regions is shown) [3]

2.3. Actuator Geometry and Material Properties

Table 1 reveals the key actuator dimensions and material properties used in the analytical model setup as well as the CFD analysis.

Table 1. Actuator geometry and material properties

Parameter	Value
Fluid dynamic viscosity	30 cP
Bulk modulus	220 MPa
Fluid density	2.5 g/cc
Area factor	1662 mm^2
Annulus size	0.7 mm
Annulus length	30 mm
Annulus area	80 mm^2
Chamber length	100 mm
No. of lumps, N	{1,3,5}

2.4. Test setup

The CFD model is exercised in such a manner to copy the testing of real shock absorbers on a hydraulic stroker, i.e., the cylinder tube is fixed while the piston is stroked with a sinusoidal constant-velocity profile at discrete frequencies (and with ever-decreasing displacement). The stroking frequencies range from 3 to 390 Hz, as the stroke is varied from the peak-to-peak value of 16 mm down to 0.12 mm at the final frequency of 390 Hz. As a consequence, the peak velocity of the driving piston is held constant at 0.15 m/s at all frequencies.

Clearly, the hydraulic network model is exercised in a manner similar to that of the CFD experiment to enable a direct comparison of the model performance against the CFD data.

2.5. Results

To analyze the influence of the number of lumps in the hydraulic network model numerical tests involving the model with N={1, 3, 5} lumps were performed within the prescribed range of input frequencies, respectively. The results are presented in Figures 9-10 as plots of the amplitude and phase angle against frequency. At first, the model was configured with the laminar model in the flow path for both piston and cylinder sections. In general, the linear approach is not satisfactory even for the relatively low speed regime considered in the study. While the linear model approaches the natural frequency of the CFD model as the number of lumps increases, the damping force amplitude at that frequency is still overestimated by a factor of 3 (for a model with 5 lumps). Therefore, the author decided to enhance the each lump with a hydraulic resistance term that is proportional to flow rate squared (Q_i^2) to account for entry/exit losses in the annulus, for example. The magnitude of these components was estimated from CFD steady-state tests. Adding the quadratic damping term improved the model. As seen in Figures 8, 9 and 10, it can be noted that the modified network model is approaching the natural frequency of the shock absorber and the amplitude as well as phase. The model, however, still overestimates the amplitude of the damping force at resonance.

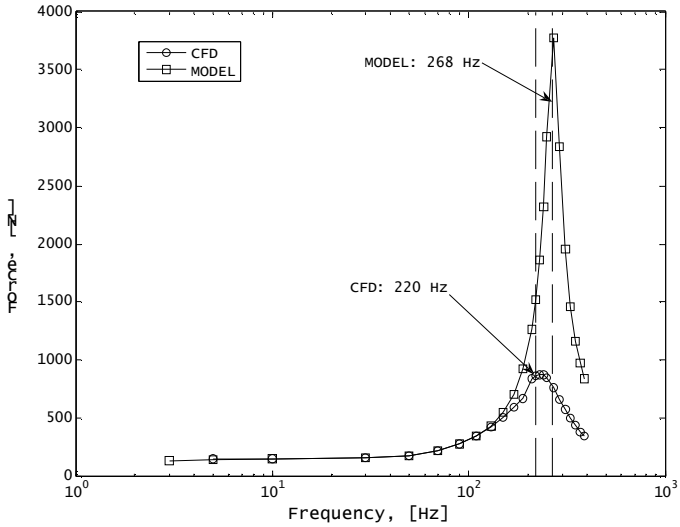

Figure 8. CFD vs. state-space model [3]

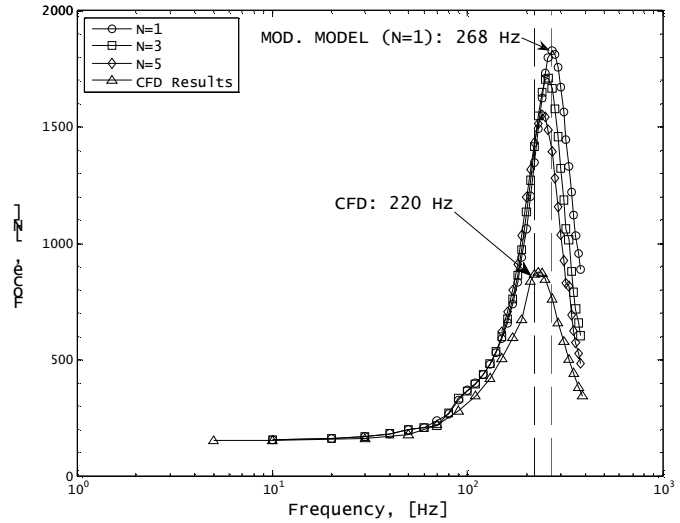

Figure 9. Force vs. frequency; modified hydraulic network model

3. SUMMARY AND CONCLUSIONS

The purpose of the paper was to illustrate the analytical model of a monotube shock absorber that is suitable for engineering purposes. That model can be used in higher frequency vehicle suspension simulations instead of more complex CFD or phenomenological models. In order to account for damping in the cylinder sections of the damper as well as fluid compressibility and inertia, the (simplified) device was modeled as a hydraulic network of lumped mass, compliance and viscous resistance elements. For comparison, the previous analytical models [1,2] assumed viscous losses only in the annulus of the piston and inviscid fluid elsewhere. When compared to the CFD experiment, the models were lightly damped. It seems the hydraulic network is better at capturing the natural frequency of the model. However, the model still overestimates the damping force at that frequency which indicates some work on the damping (viscous loss) component of the network model is still required.

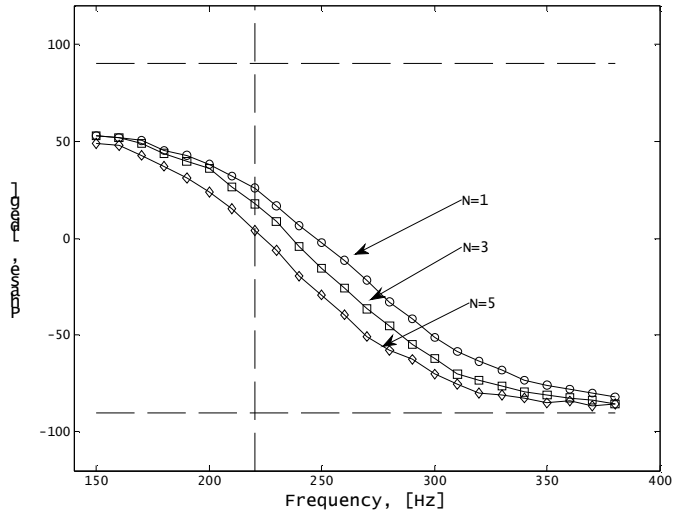

Figure 10. Phase shift vs. frequency; modified hydraulic network model

REFERENCES

1. Alexandridis A. A., Gołdasz, J.: High-frequency Dynamics of Magneto-Rheological Dampers. In: Proceedings of the Ninth International Conference on New Actuators ("ACTUATOR 2004"), Bremen, Germany, 14-16 June, 2004.
2. Alexandridis A. A, Gołdasz J.: Simplified model of the dynamics of magneto-rheological dampers. "Mechanics" 2005, Vol. 24(2), p. 47-53.
3. Gołdasz, J., Alexandridis A. A.: Frequency-dependent behavior of MR dampers: CFD Study. In: Proceedings of the Active Noise and Vibration Control Methods Conference ("MARDiH 2007"), Krasiczyn, Poland, 11-14 June, 2007.
4. Peel D. J., Stanway R., Bullough W. A.: Dynamic modeling of ER vibration damper for vehicle suspension applications. „Smart Materials and Structures" 1996, Vol. 5, p. 591-606.
5. Hopkins P. N.: Magnetorheological fluid damper. US Patent 6311810, 2001.
6. Petek, N.: Adjustable dampers using electrorheological fluids. US Patent 5259487, 1993.
7. Nguyen Q.-H., Choi S.: A new approach for dynamic modeling of an electrorheological damper using a lumped parameter method, Nguyen, Quoc-Hung; Choi, Seung-Bok, "Smart Materials and Structures" 2009, Vol. 18(11), p. 115 – 120.